Fracture Mechanics of Concrete Structures
Proceedings FRAMCOS-3
AEDIFICATIO Publishers, D-79104 Freiburg, Germany

SIMULATIONS OF SIZE EFFECT IN MASONRY STRUCTURES

P.B. Lourenço[1],
Department of Civil Engineering, University of Minho
Portugal

Abstract
The importance of size effect for the design of structures made of quasi-brittle materials is a well debated issue but discussions of size effect in masonry structures received very little attention in the literature. Here, results of the dependence of the failure load in the structural size are presented, for three different structures with different failure mechanisms. For the given structures, it is shown that collapse dominated by a tensile mechanism shows size effect and collapse dominated by a slide (shear) mechanism does not show size effect. For failure dominated by a compressive mechanism, further investigations are necessary.
Key words: Size-effect, masonry, numerical simulations

1 Introduction

Until fifteen years ago, it was generally believed that the size effect in structural failure was of statistical origin. It is now widely accepted that size effect is mostly a consequence of the softening behaviour of quasi-brittle materials, whenever failure does not occur at the initiation of cracking.

---

[1] Formerly also at Delft University of Technology, the Netherlands

Many studies, both of experimental and theoretical nature, have dealt with size effect, and an approximate size-effect law applicable to structures in which fracture is preceded by distributed cracking in a large fracture-process zone has been formulated already by Bazant (1984). A comprehensive study on the evidence of fracture size effect for concrete structures and a comparison with extensive experimental data can be found in Bazant et al. (1994) and Carpinteri et al. (1995).

The problem of size effect is particularly important to structural engineers, whom must inevitably extrapolate from reduced-scale laboratory tests to real structures. For masonry structures, the size effect issue becomes more acute because it is normal in practice to adopt unreinforced masonry, which necessarily behaves in a quasi-brittle manner. Tests performed using units with one half the real size, Page (1981), one quarter of the real size, Gergely et al. (1993), up to one sixth of the real size, Samarasinghe and Hendry (1980), are common. Additionally, and due to the internal structure of masonry, it is possible to discuss two "size-effect" aspects, one related to the ratio between nominal dimension and strength and, another, related to the ratio between unit dimension and nominal dimension. These two aspects will be discussed in this paper, via the results in a masonry pier subjected to a concentrated (point) load and masonry shear walls. The interface model adopted in the analyses is fully described in Lourenço and Rots (1997) and includes a tension cut-off, Coulomb friction model and a compression cap.

2 Pier subjected to a point load

This example consists of a masonry pier with a point load, see Fig. 1. The chosen material parameters represent typical values observed experimentally (Young´s moduli E_u = 15000 N/mm2 and E_j = 3000 N/mm^2, tensile strengths f_{tu} = 0.75 N/mm^2 and f_{tj} = 0.15 N/mm^2, fracture energies G_{fu} = 0.025 N.mm/mm^2 and G_{ft} = 0.012 N.mm/mm^2, cohesion c_j = 0.3 N/mm^2, mode II fracture G_{IIj} = 0.03 N.mm/mm^2, compressive strength f_m = 12 N/mm^2 and compressive fracture energy G_{cm} = 9 N.mm/mm^2, where the subscripts u refer to the unit, j to the joint and m to masonry), see also Lourenço (1997). The units have dimensions 140 × 50 × 100 mm^3 and the joints are 10 mm thick. Note that a non-zero fake interface thickness is used to avoid showing inter-penetration of the units. This is a representation of the true thickness of the joint that is not taken into account in the analysis. In reality, the interfaces have zero thickness and the dimensions of the continuum elements must be enlarged by the unit joint thickness. At the top of the pier, the force is applied with an infinitely rigid plate, modelled by tying the vertical displacement of the

nodes under the plate. At the bottom of the pier, the (mid-) nodes belonging to the symmetry axis are also tied to have symmetric horizontal displacements.

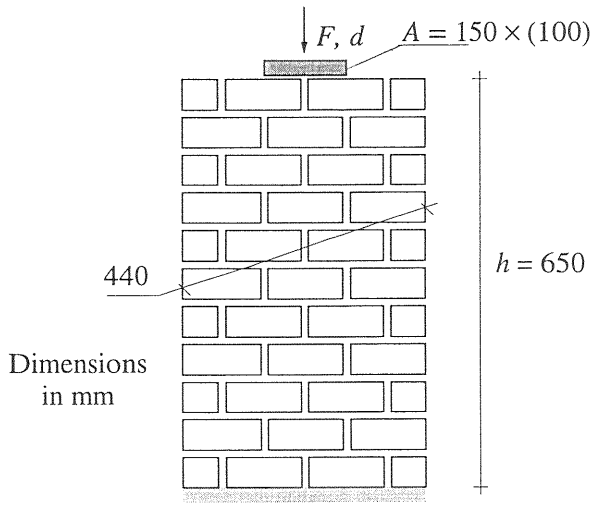

Fig. 1. Masonry pier subjected to point load

For the numerical analysis, each unit is modelled with eight quadratic plane stress elements. Interface elements are used to model the joints and potential vertical cracks placed vertically in the middle of the units. The analysis is carried out with a special arc-length control that automatically searches for the largest relative displacement in the interfaces.

The diagram for the vertical pressure F/A vs. the non-dimensional displacement of the rigid plate d/h is given in Fig. 2, where F is the vertical force in the plate, A is the area of the plate, d is the vertical displacement of the plate and h is the specimen height. The rising portion of the curve appears to be almost linear, indicating that the effect of cracking prior to reaching the maximum load is negligible. After peak load, a very sudden decrease of both the load and the displacement occurs. This very sharp snap-back obtained at peak load is due to the sudden energy release in the straight crack that arises under the load.

Fig. 3 shows total and incremental deformed meshes for different load stages. A straight vertical crack appears through head joints and units. The crack starts at the top of the specimen and progresses until its bottom. Once a critical stage is reached (peak load), the elastic energy stored in the specimen is too large and the specimen snaps to a full crack.

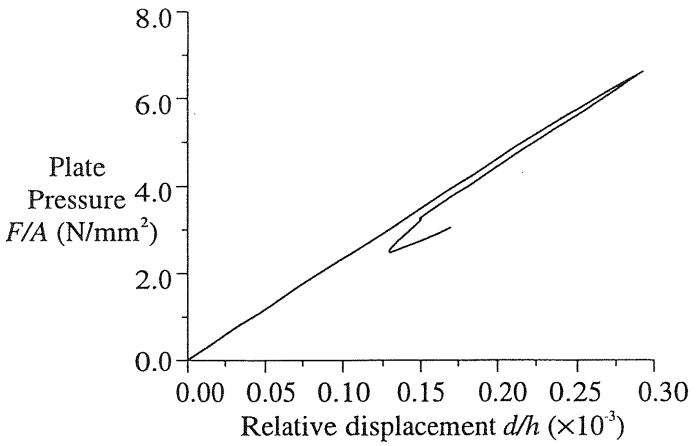

Fig. 2. Load-displacement diagram for pier subjected to point load

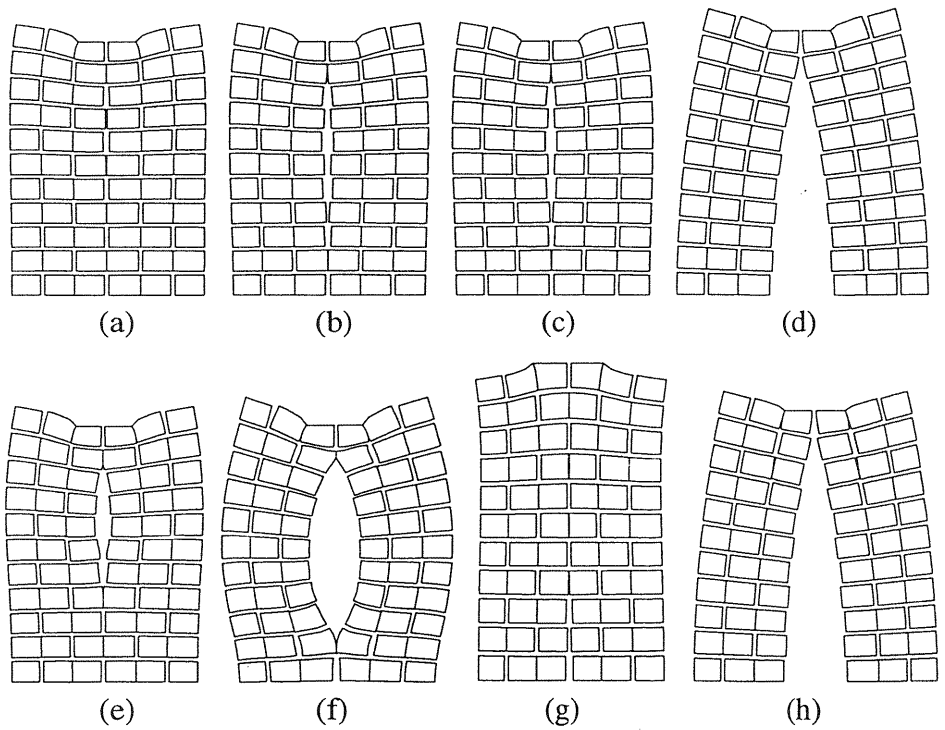

Fig. 3. Total and incremental deformed meshes for pier subjected to point load: (a,e) early stage; (b,f) just before peak; (c,g) just after peak; (d,h) ultimate stage

2.1 The ratio between nominal dimension and strength

The analysis is repeated with a similar specimen, such that the specimen size is reduced by a factor two. Fig. 4 shows that a higher nominal stress

is obtained, even if no remarkable differences are encountered in the behaviour of the structure.

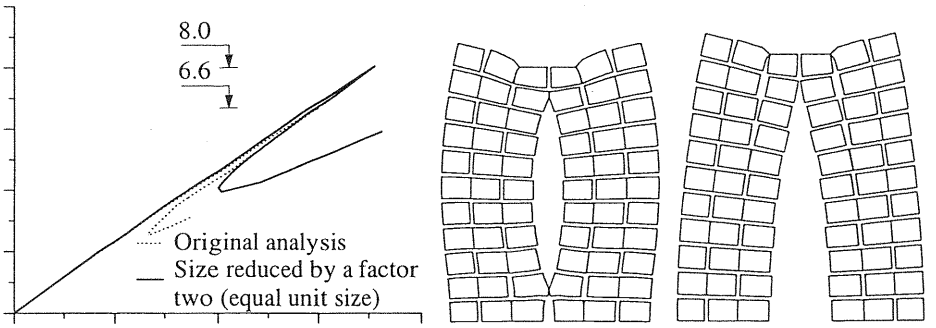

Fig. 4. Results of the analysis for a size reduced by a factor two: (a) load-displacement diagram; displacements at (b) peak and (c) failure.

The analysis is repeated again with a similar specimen, such that the specimen size is augmented by a factor two. Fig. 5 shows that a much lower nominal stress is obtained. A significant difference can be observed also in the behaviour of the structure at peak. When the structure snaps, the vertical crack in the new analysis has a much smaller development than the vertical crack in the original analysis. This illustrates well the fact that the elastic energy stored in a structure increases with the structural size, for the same deformed configuration. No significant difference is found at ultimate stage.

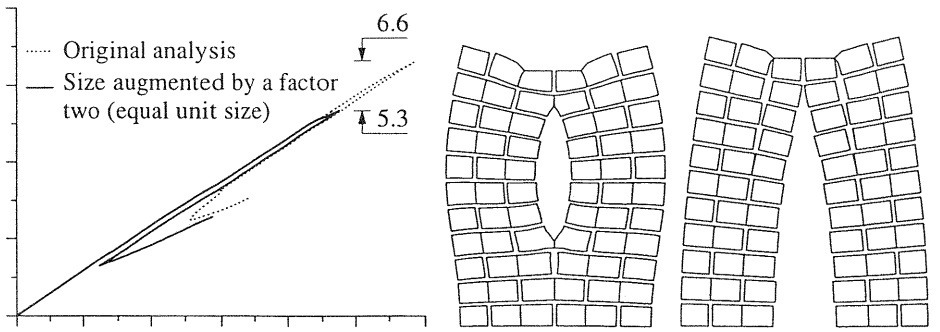

Fig. 5. Results of the analysis for a size augmented by a factor two: (a) load-displacement diagram; displacements at (b) peak and (c) failure.

Finally, the analysis is repeated, such that the specimen size is augmented by a factor four. Fig. 6 shows that the nominal stress reduces further. The difference observed in the behaviour of the structure at peak becomes more severe as the structure snaps once the second unit counting from the top cracks. No significant difference is found at ultimate stage.

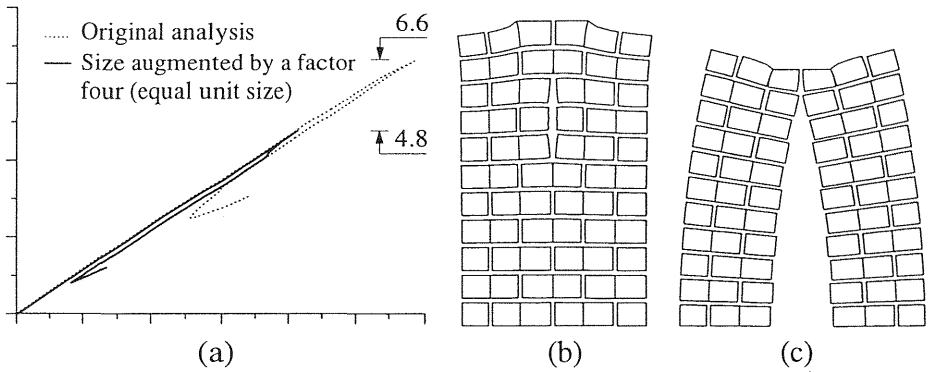

Fig. 6. Results of the analysis for a size augmented by a factor four: (a) load-displacement diagram; displacements at (b) peak and (c) failure.

The analysis has been repeated for different structural sizes, namely 1.5, 2.5, 3 and 3.5 times the original size. It was found, Lourenço (1997), that the elastic stiffness as well as the ultimate stiffness, obtained once the full vertical crack is retrieved, are exactly the same for all the examples. Nevertheless, significantly different peak loads are obtained. The values of the collapse loads are summarised in Fig. 7, which clearly shows the reduction of strength with the structural size in the usual logarithmic scale. The size effect law proposed by Bazant (1984) does not seem to fit the values well for larger structural sizes because the failure tends to a constant non-zero value. Therefore, the multifractal scaling law of Carpinteri et al. (1995) gives better agreement.

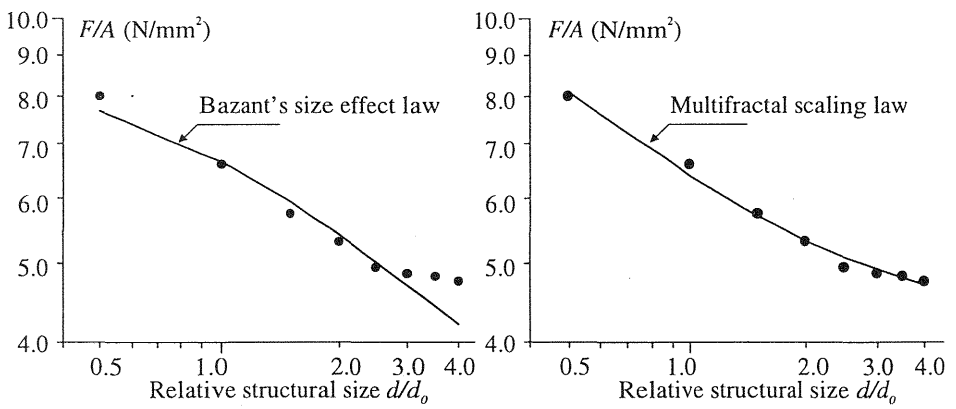

Fig. 7. Nominal stress vs. structural size. Comparison of results with (a) Bazant's size effect law and (b) multifractal scaling law

2.2 The ratio between nominal dimension and unit dimension

Next, the analysis is repeated with a specimen of the same size, but with an increasing number of units. Fig. 8 shows the results for an analysis

with the double number of units, i.e. the unit and joint size is reduced by a factor two. It can be observed that the structural response remains approximately constant, both in terms of stiffness and peak load. The small difference found is probably explained by the larger number of integration points in the crack propagation zone. Again, no relevant differences are found between the original analysis and the new analysis.

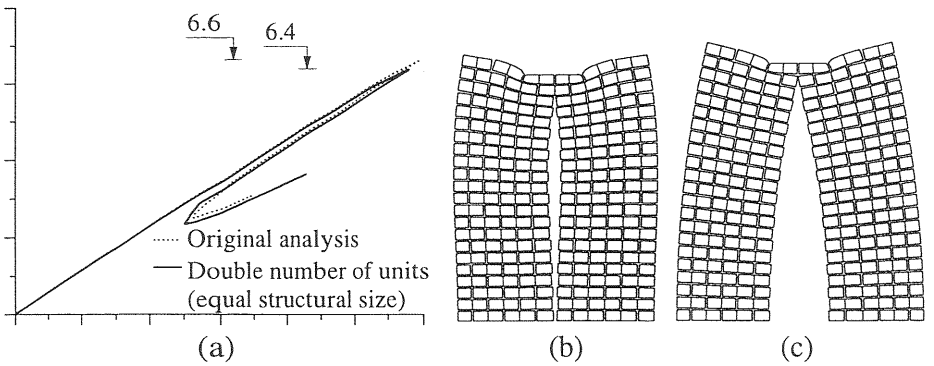

Fig. 8. Results of the analysis for the double number of units:
(a) load-displacement diagram; displacements at (b) peak and (c) failure.

Fig. 9 shows the load-displacement diagram for an analysis with four times the number of units. The response is even closer to the response with a double number of units, which seems to confirm a certain asymptotic behaviour towards a unique solution upon "size refinement".

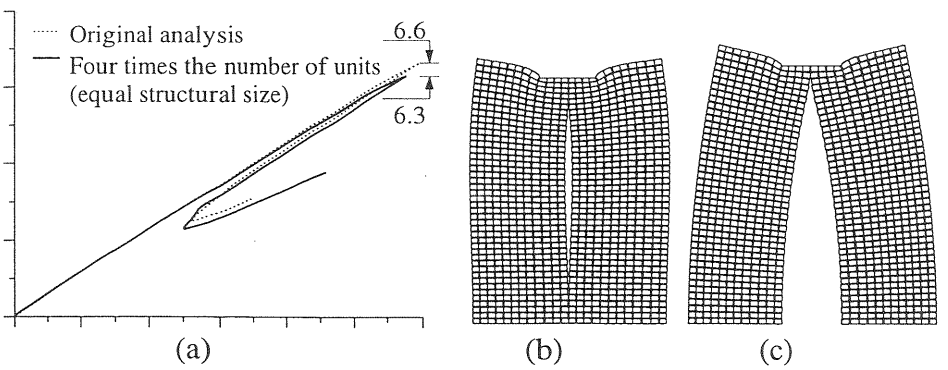

Fig. 9. Results of the analysis for four times the number of units:
(a) load-displacement diagram; displacements at (b) peak and (c) failure.

3 Shear wall with an opening (top edge free)

The next example consists of a masonry shear wall with an opening. An initial vertical load p = 1.0 N/mm^2 is applied before shearing the wall with the horizontal force F. The top boundary remains horizontal but can

move freely in the vertical direction. The points in the top boundary are constrained to have the same horizontal displacement d. The opening in the centre of the wall forces the compressive strut, which arises during loading, to spread around it. At collapse, four rigid blocks are formed.

The diagram for the non-dimensional horizontal "shear" force *F/A* vs. the non-dimensional displacement of the rigid plate *d/b* is given in Fig. 10, where *F* is the horizontal force applied to the structure, *A* is the area of a horizontal cross section of the wall close to the boundaries, *d* is the horizontal displacement of the top edge and *b* is the specimen width. A very ductile type of failure was encountered. The perfect plateau obtained indicates that a shear failure was obtained corresponding to the dry friction retrieved once the cohesion is exhausted.

No dependence of the results on the structural size is found.

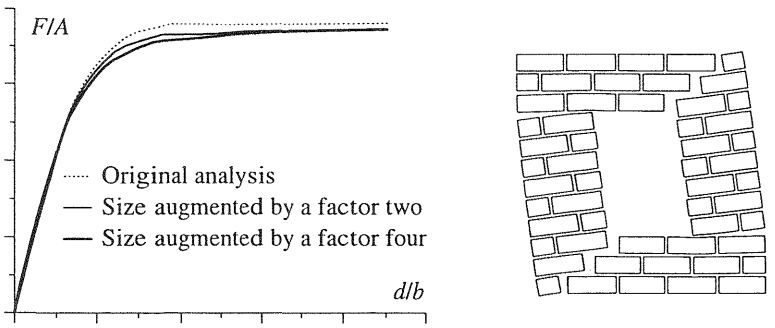

(a) (b)

Fig. 10. Results of the analysis for shear wall (top edge free): (a) load-displacement diagram; (b) deformed mesh at failure.

4 Shear wall with an opening (top edge restrained)

To finalise this study, a third example is analysed, which is similar to the previous one, with the exception of the top boundary, which is not allowed to move vertically during horizontal shearing. This increases the vertical confining pressure due to dilatancy. Therefore, the normal stress increase contributes to masonry crushing in the compressed toes.

The diagram for the non-dimensional horizontal "shear" force *F/A* vs. the non-dimensional displacement of the rigid plate *d/b* is given in Fig. 11. A ductile type of failure was still encountered, even if some post-peak softening is visible in the response. Crushing in the compressed toes of the wall was already initiated at the stage where the analysis was stopped.

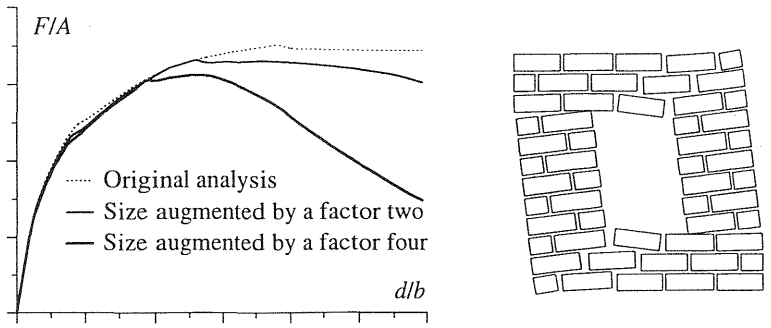

(a) (b)

Fig. 11. Results of the analysis for shear wall (top edge restrained): (a) load-displacement diagram; (b) deformed mesh at failure.

Size effect is found and, for the larger structure, the nominal strength was reduced by 13%. The after-peak behaviour is also different and the response is less ductile than the original response. This can be explained by the elastic energy stored in the body, which becomes too large for the fracture energy available at the crushed toes. Similar failure mechanisms were obtained in all the cases and the justification for the differences in the analysis cannot be attributed to a different failure mechanism.

This "compressive size effect" is not novel, Bazant and Xiang (1997). Nevertheless, the present results represent only a first attempt to discuss the problem because compressive failure is quite complex, with contributions of local and non-local nature, Vonk (1992). It is questionable if the adopted modelling for compressive failure (only of local nature) is adequate to accurately study size effect phenomena.

5 Conclusions

The present paper addresses size effect in masonry structures, which seems to be not a well debated issue in the literature. Three different structures are analysed: a pier subjected to a point load, a shear wall with a unconstrained top edge and a shear wall with a constrained top edge. The first structure features a tension dominant failure, the second structure features a shear dominant failure and the third structure features a compressive dominant failure.

In the case of tension failure, the size effect is significant and follows the multifractal scaling law of Carpinteri et al. (1995). In case of shear failure, a perfectly plastic solution is obtained and the size effect is negligible. In case of compressive failure, the size effect becomes again important. Additional studies are necessary because the adopted model for compressive failure is only of local nature.

6 Acknowledgements

This research has been supported financially by the Netherlands Technology Foundation (STW) under grant DCT 33.3052. The author gratefully acknowledges the support of the project leader Dr. Jan G. Rots, from TNO Building and Construction Research, the Netherlands.

7 References

Bazant, Z.P. (1984) Size effect in blunt failure: concrete, rock, metal. **J. Engrg. Mech.**, ASCE, 110(4), 518-535.

Bazant, Z.P. and Xiang, Y. (1997) Size effect in compression fracture: Splitting crack band propagation. **J. Engrg. Mech.**, ASCE, 123(2), 162-172.

Bazant, Z.P., Ozbolt, J. and Eligehausen, R. (1994) Fracture size effect: review of evidence for concrete structures. **J. Struc. Mech.**, ASCE, 120(8), 2377-2398.

Carpinteri, A, Chiaia, B. and Ferro, G. (1995) **Multifractal scaling laws: an extensive application to nominal strength size effect of concrete structures**. Report n° 51. Politecnico di Torino, Turin, Italy.

Gergerly, P., White, R.N., Zawilinski, D. and Mosalam, K. (1993) The interaction of masonry in-fill and steel or concrete frames, in **Nat. Earthquake Conf.**, USA, 2, 183-191.

Lourenço, P.B. (1997) **Two aspects related to the analysis of masonry structures: Size effect and parameter sensitivity**. Report n° 03.21.1.31.25. Delft Univ. of Tech., Delft, The Netherlands.

Lourenço, P.B. and Rots, J.G. (1997) A multi-surface interface model for the analysis of masonry structures. **J. Engrg. Mech.**, ASCE, 123(7), 660-668.

Page, A.W. (1981) The biaxial compressive strength of brick masonry. **Proc. Instn. Civil Engrs.**, Part 2, 71, 893-906.

Samarasinghe, W. and Hendry, A.W. (1980) The strength of brickwork under biaxial tensile and compressive stress, in **7th Int. Symp. on Load Bearing Brickwork**, London, UK, 129-140.

Vonk, R.A. (1992) **Softening of concrete loaded in compression**. Dissertation, Eindhoven Univ. of Tech., Eindhoven, The Netherlands.